Modelling Simul. Mater. Sci. Eng. **4** (1996) 137–150. Printed in the UK

Electronic and atomic structure of liquid potassium via path integral molecular dynamics with non-local quantum exchange

P A Deymier, G E Jabbour, J D Weinberg and F J Cherne

Department of Materials Science and Engineering, University of Arizona, Tucson, AZ 85721, USA

Received 11 May 1995, in final form 31 October 1995

Abstract. We develop a novel first-principle molecular dynamics method based on the discretized path integral formalism of quantum mechanics. This method which includes quantum exchange is used to simulate the behavior of liquid potassium at high temperature. We compute the energy as well as the electronic and atomic structural properties of the liquid metal. These results compare favorably with previous calculations and experimental results.

1. Introduction

Molecular dynamics is a useful technique for the study of solids and liquids [1]. Over the past decade, there has been a great deal of effort and progress directed toward implementing first-principle molecular dynamics. For example, the Car and Parrinello method [2] based on density functional theory has been successfully employed to simulate a large variety of systems. Among these, liquid alkali metals have received a good deal of attention [3, 4]. Alkali metals are good prototypes of free-electron systems which offer a particular challenge due to the intimate relation and cooperative evolution of the atomic and electronic structure.

It is easy for liquids to undergo local density fluctuations in response to some electronic change [5]. For instance, a metal/non-metal transition in expanded alkali metals can be seen near the liquid–gas critical density [6]. It has been speculated that density inhomogeneities in the form of clusters are associated with such transitions [7]. The strong correlation between the structure of the liquid and the electronic structure necessitates a theoretical study that is capable of determining the correlated electronic structure. Furthermore, the possibility for the electronic structure to change from delocalized electrons to localized electrons suggests the use of a method based on a complete set of states such as in a position representation. This method should also allow for the study of finite temperature properties including ionic motion.

We report in this paper an investigation of the structure of liquid potassium using a new molecular dynamics method which incorporates the above-mentioned requirements. In our system, which is composed of ionic and electronic degrees of freedom, the ionic degrees of freedom are described classically. The electronic degrees of freedom, meanwhile, are described via the path integral formulation of quantum statistical mechanics. In the discretized path integral formulation the quantum problem is shown to be isomorphic to an appropriate classical problem [8]. In absence of exchange each electron is mapped onto a

0965-0393/96/020137+14$19.50

closed necklace composed of P nodes interacting through appropriate harmonic forces. The necklace is isomorphic to the path of the electron in imaginary time. In order to simulate exchange between electrons, the direct simulation of fermionic degrees of freedom using the discretized path integral representation should include crosslinking of the necklaces [9]. The simulation of fermionic systems is complicated by the negative weights in the partition function resulting from the crosslinking of even numbers of necklaces corresponding to even permutations of electrons. Recently, Hall proposed an approximate form of the many-electron short time propagator used in path integral simulations that includes the effects of exchange [10–12]. Similar to the approach of Hall, an effective classical potential, which includes the effects of exchange, is implemented in the molecular dynamics algorithm. This effective potential gives rise to a repulsive barrier between isospin electrons which ensures that the Pauli exclusion principle is upheld. The calculated electronic structure of the liquid metal is characterized by a spin-dependent pair distribution function as well as the kinetic energy of the electrons. We demonstrate that our exchange potential is quite effective in enforcing spatial exclusion of isospin electrons resulting in more localized states. Our results also show reasonable agreement between the calculated K–K pair distribution function and experimental ones.

The paper is organized as follows. In section 2, we derive an effective exchange potential which allows the simulation of indistinguishable quantum particles with the method of molecular dynamics. Both the model system and details on the practical implementation of this method are given in this section. Section 3 contains the results of our simulations of liquid potassium as well as a discussion of the liquid and electronic structures. Finally, some conclusions are drawn regarding the applicability of the technique to other systems.

2. Method and model

2.1. Method

The quantum statistical partition function for a single particle may be written as [13]

$$Z = \int \mathrm{d}\boldsymbol{r}_1 \, \langle \boldsymbol{r}_1 | \mathrm{e}^{-\beta H_{\mathrm{op}}} | \boldsymbol{r}_1 \rangle \approx \lim_{P \to \infty} \int \mathrm{d}\boldsymbol{r}_1 \, \langle \boldsymbol{r}_1 | (\mathrm{e}^{-\beta H_{\mathrm{op}}/P})^P | \boldsymbol{r}_1 \rangle \tag{1}$$

where H_{op} is the Hamiltonian operator for our system and is a sum of the kinetic and potential operators. β is $1/kT$. By substituting $\tau = -\mathrm{i}\hbar\beta$ in equation (1), one can think of the Boltzmann factor, $\exp(-\beta H_{\mathrm{op}})$, as the time evolution operator of the classical particle in imaginary time space.

Upon introducing $(P-1)$ intermediate states in Z, we obtain the path integral representation of the partition function

$$Z \approx \int \mathrm{d}\boldsymbol{r}_1 \, \mathrm{d}\boldsymbol{r}_2 \ldots \mathrm{d}\boldsymbol{r}_P \, \langle \boldsymbol{r}_1 | \mathrm{e}^{-\epsilon H_{\mathrm{op}}} | \boldsymbol{r}_2 \rangle \langle \boldsymbol{r}_2 | \mathrm{e}^{-\epsilon H_{\mathrm{op}}} | \boldsymbol{r}_3 \rangle \ldots \langle \boldsymbol{r}_P | \mathrm{e}^{-\epsilon H_{\mathrm{op}}} | \boldsymbol{r}_1 \rangle \tag{2}$$

where $\epsilon = \beta/P$.

In equation (2), the first term represents the path from $\boldsymbol{r}_1$ to $\boldsymbol{r}_2$, the second connects $\boldsymbol{r}_2$ to $\boldsymbol{r}_3$, and so on. Notice that the last term in this equation connects $\boldsymbol{r}_P$ to $\boldsymbol{r}_1$, thus closing the overall path. In other words, the single quantum particle is now transformed to look like a polymeric necklace consisting of P beads or nodes. With the periodic boundary condition (cyclic condition)

$$\boldsymbol{r}_{P+1} = \boldsymbol{r}_1. \tag{3}$$

We can rewrite the partition function in a more compact form

$$Z \approx \int \prod_{n=1}^{P} \mathrm{d}\boldsymbol{r}_n \, \langle \boldsymbol{r}_n | \mathrm{e}^{-\epsilon H_{\mathrm{op}}} | \boldsymbol{r}_{n+1} \rangle. \tag{4}$$

Using the Trotter formula, the propagator could be approximated as follows [14]:

$$\langle \boldsymbol{r}_n | \mathrm{e}^{-\epsilon H_{\mathrm{op}}} | \boldsymbol{r}_{n+1} \rangle \approx \langle \boldsymbol{r}_n | \mathrm{e}^{-\epsilon T_{\mathrm{op}}} \mathrm{e}^{-\epsilon \Phi_{\mathrm{op}}} | \boldsymbol{r}_{n+1} \rangle \tag{5}$$

where T_{op} is the kinetic energy operator and Φ_{op} is a potential operator. In the case of a local potential operator and introducing the closure relation in equation (5), the partition function of a single particle becomes [14]

$$Z \approx \int \prod_{n=1}^{P} \mathrm{d}\boldsymbol{r}_n \, \langle \boldsymbol{r}_n | \mathrm{e}^{-\epsilon T_{\mathrm{op}}} | \boldsymbol{r}_{n+1} \rangle \exp\left[-\frac{\beta}{P} \sum_{i=1}^{P} \Phi(\boldsymbol{r}_i) \right]. \tag{6}$$

In equation (6), $\Phi(\boldsymbol{r})$, represents some potential function of the position. The term in brackets is simply the free-particle density matrix [13], which may be written as

$$\langle \boldsymbol{r}_n | \mathrm{e}^{-\beta T_{\mathrm{op}}/P} | \boldsymbol{r}_{n+1} \rangle = \left[\frac{Pm}{2\pi\beta\hbar^2} \right]^{3/2} \exp\left[-\beta \frac{Pm}{2\beta^2\hbar^2} (\boldsymbol{r}_n - \boldsymbol{r}_{n+1})^2 \right] \tag{7}$$

with m being the mass of the particle.

The quantum partition function is isomorphic to a classical partition function which takes the form

$$Z \approx \left[\frac{Pm}{2\pi\hbar^2\beta} \right]^{3P/2} \int \prod_{n=1}^{P} \mathrm{d}\boldsymbol{r}_n \, \exp(-\beta V_{\mathrm{eff}}(\boldsymbol{r}_1, \ldots, \boldsymbol{r}_P)) \tag{8}$$

with

$$V_{\mathrm{eff}}(\boldsymbol{r}_1, \ldots, \boldsymbol{r}_P) = \sum_{i=1}^{P*} \left[\frac{Pm}{2\hbar^2\beta^2} (\boldsymbol{r}_i - \boldsymbol{r}_{i+1})^2 + \frac{1}{P} \Phi(\boldsymbol{r}_i) \right]. \tag{9}$$

The '$*$' denotes the cyclic condition. The quantum particle may, therefore, be represented by a necklace of P nodes such that a point in the necklace interacts with its first neighbors in the chain through a harmonic potential of spring constant $C = (Pm/\hbar^2\beta^2)$. The isomorphism between the quantum and classical representations becomes more accurate as $P \to \infty$.

Equation (8) can be generalized to represent more than one quantum particle. The partition function of a collection of N, interacting quantum particles in absence of quantum exchange, is written as

$$Z \approx \left[\frac{1}{N!} \right]^P \left[\frac{Pm}{2\pi\hbar^2\beta} \right]^{3NP/2} \int \prod_{j=1}^{N} \prod_{i=1}^{P} \mathrm{d}\boldsymbol{r}_i^{(j)} \, \exp\left[-\beta \sum_{j=1}^{N} \sum_{i=1}^{P*} \frac{Pm}{2\hbar^2\beta^2} (\boldsymbol{r}_i^{(j)} - \boldsymbol{r}_{i+1}^{(j)})^2 \right]$$
$$\times \exp\left[-\frac{\beta}{P} \sum_{j=1}^{N} \sum_{i=1}^{P} \Phi(\boldsymbol{r}_i^{(j)}) \right] \times \exp\left[-\frac{\beta}{P} \sum_{j>k}^{N} \sum_{i=1}^{P} \Psi_{jk}(\boldsymbol{r}_i^{(j)} - \boldsymbol{r}_i^{(k)}) \right]. \tag{10}$$

The potential $\Psi_{jk}(\boldsymbol{r}_i^{(j)} - \boldsymbol{r}_i^{(k)})$ accounts for the interaction between the particles. In the case of a Coulombic interaction,

$$\Psi_{jk}(\boldsymbol{r}_i^{(j)} - \boldsymbol{r}_i^{(k)}) = \frac{\mathrm{e}^2}{4\pi\epsilon_0 |\boldsymbol{r}_i^{(j)} - \boldsymbol{r}_i^{(k)}|}. \tag{11}$$

In this form the particles 'j' and 'k' can only interact when in the same discrete quantum state (or at the same imaginary time) as indicated by the subscript 'i'.

Equation (10) acquires further complications upon the inclusion of exchange. This is due to the formation of dimers, trimers, and higher-order 'polymeric' structures that arise from the 2-cycle, 3-cycle, and up to N-cycle permutations of particles. These contributions appear in the form of extra terms in the partition function. The quantum partition function of a system composed of interacting electrons (fermions) including exchange is given by [9]

$$Z \approx \left[\frac{1}{N!}\right]\left[\frac{Pm}{2\pi\overline{h}^2\beta}\right]^{3NP/2}\int\prod_{j=1}^{N}\prod_{i=1}^{P}\mathrm{d}\boldsymbol{r}_i^{(j)}M[A_{n,n+1}]\exp\left[-\frac{\beta}{P}\sum_{j=1}^{N}\sum_{i=1}^{P}\Phi(\boldsymbol{r}_i^{(j)})\right]$$
$$\times\exp\left[-\frac{\beta}{P}\sum_{j>k}^{N}\sum_{i=1}^{P}\Psi_{jk}(\boldsymbol{r}_i^{(j)}-\boldsymbol{r}_i^{(k)})\right]. \tag{12}$$

The term $M[A_{n,n+1}]$ stands for the determinant of an $N\times N$ matrix whose elements are given by

$$A_{n,n+1}^{jk}\propto\langle\boldsymbol{r}_n^{(j)}|\mathrm{e}^{-\beta T_{\mathrm{op}}/P}|\boldsymbol{r}_{n+1}^{(k)}\rangle \tag{13}$$

where

$$\langle\boldsymbol{r}_n^{(j)}|\mathrm{e}^{-\beta T_{\mathrm{op}}/P}|\boldsymbol{r}_{n+1}^{(k)}\rangle=\left[\frac{Pm}{2\pi\beta\overline{h}^2}\right]^{3/2}\exp\left[-\beta\frac{Pm}{2\beta^2\overline{h}^2}(\boldsymbol{r}_n^{(j)}-\boldsymbol{r}_{n+1}^{(k)})^2\right]. \tag{14}$$

In the absence of quantum exchange the determinant is

$$M[A_{n,n+1}]=\prod_{j=1}^{N}A_{n,n+1}^{jj} \tag{15}$$

and equation (12) reduces to equation (10). The off-diagonal element of the matrix $[A_{n,n+1}]$, $A_{n,n+1}^{jk}$, represents a path from $\boldsymbol{r}_n^{(j)}$ to $\boldsymbol{r}_{n+1}^{(k)}$. This path is associated with a permutation between particle 'j' and 'k'.

To develop exchange further, we rewrite the matrix $[A_{n,n+1}]$ in the form:

$$[A_{n,n+1}]=[F_{n,n+1}]\times[E_{n,n+1}] \tag{16}$$

where

$$F_{n,n+1}^{ij}=\begin{cases}0 & \text{if } i\neq j\\ A_{n,n+1}^{jj} & \text{if } i=j\end{cases}$$

and

$$E_{n,n+1}^{ij}=\exp\left[-\beta\frac{Pm}{2\beta^2\overline{h}^2}[(\boldsymbol{r}_n^{(i)}-\boldsymbol{r}_{n+1}^{(j)})^2-(\boldsymbol{r}_n^{(i)}-\boldsymbol{r}_{n+1}^{(i)})^2]\right]. \tag{17}$$

To illustrate this step we consider the case of two fermions. Equation (16) may be written as

$$\begin{pmatrix}A_{n,n+1}^{11} & A_{n,n+1}^{12}\\ A_{n,n+1}^{21} & A_{n,n+1}^{22}\end{pmatrix}=\begin{pmatrix}F_{n,n+1}^{11} & F_{n,n+1}^{12}\\ F_{n,n+1}^{21} & F_{n,n+1}^{22}\end{pmatrix}\begin{pmatrix}E_{n,n+1}^{11} & E_{n,n+1}^{12}\\ E_{n,n+1}^{21} & E_{n,n+1}^{22}\end{pmatrix}. \tag{18}$$

We now drop the indices n and $n+1$ for simplicity. If we define

$$[F]=\begin{pmatrix}A^{11} & 0\\ 0 & A^{22}\end{pmatrix} \tag{19}$$

as is done in the second part of equation (16), then the matrix $[E]$ has to take the form

$$[E]=\begin{pmatrix}\frac{A^{11}}{A^{11}} & \frac{A^{12}}{A^{11}}\\ \frac{A^{21}}{A^{22}} & \frac{A^{22}}{A^{22}}\end{pmatrix}. \tag{20}$$

Since the elements, A^{jk}, are defined in equations (13) and (14) as

$$A^{jk}_{n,n+1} \propto \exp\left[-\beta\frac{Pm}{2\beta^2\hbar^2}(\boldsymbol{r}_n^{(j)} - \boldsymbol{r}_{n+1}^{(k)})^2\right]$$

the matrix $[E]$ is, therefore, composed of ones on the diagonal and exponential (equation (17)) off the diagonal. With this, $M[A_{n,n+1}]$ becomes

$$M[A_{n,n+1}] = \prod_{j=1}^{N} A^{jj}_{n,n+1} \times M[E_{n,n+1}] \tag{21}$$

where the second term contains all the exchange effects. The determinants $M[E_{n,n+1}]$ and $M[A_{n,n+1}]$ generally contain terms with negative weight when the length of the exchange permutation cycle is made up of even numbers of particles [13].

For instance, the expression for $M[E_{n,n+1}]$ may be rewritten in the form

$$\begin{aligned} M[E_{n,n+1}] = 1 &- \sum_i \sum_j \exp\Bigg[-\beta\frac{C}{2}((\boldsymbol{r}_n^{(i)} - \boldsymbol{r}_{n+1}^{(j)})^2 + (\boldsymbol{r}_n^{(j)} - \boldsymbol{r}_{n+1}^{(i)})^2 \\ &-(\boldsymbol{r}_n^{(i)} - \boldsymbol{r}_{n+1}^{(i)})^2 - (\boldsymbol{r}_n^{(j)} - \boldsymbol{r}_{n+1}^{(j)})^2)\Bigg] \\ &+ \sum_i \sum_j \sum_k \exp\Bigg[-\beta\frac{C}{2}((\boldsymbol{r}_n^{(i)} - \boldsymbol{r}_{n+1}^{(j)})^2 + (\boldsymbol{r}_n^{(j)} - \boldsymbol{r}_{n+1}^{(k)})^2 + (\boldsymbol{r}_n^{(k)} - \boldsymbol{r}_{n+1}^{(i)})^2 \\ &-(\boldsymbol{r}_n^{(i)} - \boldsymbol{r}_{n+1}^{(i)})^2 - (\boldsymbol{r}_n^{(j)} - \boldsymbol{r}_{n+1}^{(j)})^2 - (\boldsymbol{r}_n^{(k)} - \boldsymbol{r}_{n+1}^{(k)})^2)\Bigg] - \cdots \end{aligned} \tag{22}$$

where the second term in this equation corresponds to exchange between pairs of electrons, while the third term corresponds to a 3-cycle exchange or simultaneous exchange among three electrons, and so on.

The difficulty in defining an effective potential resides in the fact that the partition function, through $M[E_{n,n+1}]$, is a sum over terms which can be either positive or negative. In order to produce an effective classical potential useful in a computer simulation, one would like to rewrite (or approximate) the partition function in a way that corresponds to a sum of positive terms. Such an approximation may be possible for some systems provided the terms with positive weight dominate the negative ones.

For instance, Monte Carlo simulations of a two-dimensional non-interacting system constituted of two polarized fermions in a harmonic potential have been reported [15]. In this study, two sampling methods were used, namely the usual importance sampling of particle permutation and coordinates, and a sampling based on weight functions including explicitly the determinant, $M[A_{n,n+1}]$. Both weight functions can take negative values; however, the fraction of states with negative signs sampled by the determinant method is much smaller. At high temperatures, the ratio of negative signs becomes very small. At fixed PT, this fraction increases with decreasing temperature.

In a more recent study, path integral calculations of a fermion system of liquid ^{3}He atoms in the normal state indicate that a restriction of the paths to a region of phase space with a positive density matrix gives reasonable results at relatively high temperatures above 1 K [16]. Considering the heavy mass of ^{3}He atoms, 1 K falls in the high-temperature region. These two studies suggest that under conditions of high temperature, we may be able to restrict phase space to a region of positive determinant.

In our case, at high temperature, the sum over pairs of fermions in equation (22) is expected to dominate. The sign of $M[E_{n,n+1}]$ is, therefore, determined by the magnitude of $(\boldsymbol{r}_n^{(i)} - \boldsymbol{r}_{n+1}^{(j)})^2$, $(\boldsymbol{r}_n^{(j)} - \boldsymbol{r}_{n+1}^{(i)})^2$ and $(\boldsymbol{r}_n^{(i)} - \boldsymbol{r}_{n+1}^{(i)})^2$, $(\boldsymbol{r}_n^{(j)} - \boldsymbol{r}_{n+1}^{(j)})^2$.

For interacting fermions, the Coulombic repulsion between the electrons dictates the distance between nodes in their respective necklaces. The distance between two successive nodes within a necklace decreases as the number of nodes P increases. At high effective temperature PT, that is high temperature and/or large number of nodes P, the large classical force constant C imposes $|\boldsymbol{r}_n^{(i)} - \boldsymbol{r}_{n+1}^{(j)}|$ and $|\boldsymbol{r}_n^{(j)} - \boldsymbol{r}_{n+1}^{(i)}|$ to be greater than $|\boldsymbol{r}_n^{(i)} - \boldsymbol{r}_{n+1}^{(i)}|$ and $|\boldsymbol{r}_n^{(j)} - \boldsymbol{r}_{n+1}^{(j)}|$ leading to a topological constraint on the sign of $(\boldsymbol{r}_n^{(i)} - \boldsymbol{r}_{n+1}^{(j)})^2 + (\boldsymbol{r}_n^{(j)} - \boldsymbol{r}_{n+1}^{(i)})^2 - (\boldsymbol{r}_n^{(i)} - \boldsymbol{r}_{n+1}^{(i)})^2 - (\boldsymbol{r}_n^{(j)} - \boldsymbol{r}_{n+1}^{(j)})^2$.

In other words, under these conditions, the Coulombic interaction breaks the symmetry between a path within a necklace and a path between different necklaces. Since the partition function is independent of the number of nodes for sufficiently large values, we may conveniently choose P such that positive determinants are the major contributors to Z. Thus, we approximate the partition function by

$$Z \cong \left(\frac{1}{N!}\right)^P \left[\frac{Pm}{2\pi\beta\hbar^2}\right]^{3NP/2} \int_{>0} \prod_{j=1}^{N}\prod_{i=1}^{P} \mathrm{d}\boldsymbol{r}_i^{(j)} \exp[-\beta V'_{\mathrm{eff}}] \exp\left[-\frac{\beta}{P}\sum_{j=1}^{N}\sum_{i=1}^{P}\Phi(\boldsymbol{r}_i^{(j)})\right] \times \exp\left[-\frac{\beta}{P}\sum_{j>k}^{N}\sum_{i=1}^{P}\Psi_{jk}(\boldsymbol{r}_i^{(j)} - \boldsymbol{r}_i^{(k)})\right] \tag{23}$$

where the $\int_{>0}$ is limited to configurations with $M[E_{n,n+1}] > 0$.

In equation (23), V'_{eff} is an effective potential which accounts for quantum exchange and is given by

$$V'_{\mathrm{eff}} = \sum_{j=1}^{N}\sum_{i=1}^{P}{}^{*}\frac{C}{2}(\boldsymbol{r}_i^{(j)} - \boldsymbol{r}_{i+1}^{(j)})^2 - \frac{1}{\beta}\sum_{n=1}^{P}{}^{*}\ln(M[E_{n,n+1}]). \tag{24}$$

Following Hall [10], we rewrite the exchange potential in a nonlocal form,

$$V'_{\mathrm{eff}} = \sum_{j=1}^{N}\sum_{i=1}^{P}{}^{*}\frac{C}{2}(\boldsymbol{r}_i^{(j)} - \boldsymbol{r}_{i+1}^{(j)})^2 - \frac{1}{\beta}\sum_{m=1}^{P}{}^{*}\sum_{n=1}^{P}{}^{*}\frac{1}{P}\ln(M[E_{n,m}]) \tag{25}$$

which allows exchange between particles at any two imaginary times (nodes) in either necklace. This procedure is, in a sense, equivalent to a mean-field approximation.

According to Hall's scheme, the exchange potential between two electrons (i) and (j) is given as

$$V_{\mathrm{exch}}^{(i)(j)} = -\frac{1}{\beta}\sum_{n=1}^{P}{}^{*}\sum_{m=1}^{P}{}^{*}\ln\left\{1 - \exp\left[-\beta\frac{Pm}{2\beta^2\hbar^2}\alpha|(\boldsymbol{r}_n^{(i)} - \boldsymbol{r}_m^{(j)})^2 + (\boldsymbol{r}_n^{(j)} - \boldsymbol{r}_m^{(i)})^2 - (\boldsymbol{r}_n^{(i)} - \boldsymbol{r}_m^{(i)}) - (\boldsymbol{r}_n^{(j)} - \boldsymbol{r}_m^{(j)})^2|\right]\right\} \tag{26}$$

where the absolute value is introduced to ensure only positive weights in the partition function. This approximation understimates the contribution of configurations with negative arguments of the exponential. Hall introduces a coefficient $\alpha \leqslant 1$ to correct for errors arising from the approximation. By contrast, our effective exchange potential is only limited to $M[E_{n,m}] > 0$ which allows for the inclusion of terms where $E_{n,m}^{ij} > 1$ or configurations such that $(\boldsymbol{r}_n^{(i)} - \boldsymbol{r}_m^{(j)})^2 - (\boldsymbol{r}_n^{(i)} - \boldsymbol{r}_m^{(i)})^2 < 0$. Since the exchange must be repulsive (to satisfy Pauli's principle), we must also restrict it to $M[E_{n,m}] \leqslant 1$. To accomplish this, $M[E_{n,m}]$ is redefined as the determinant of $[E_{n,m}]$ when $M[E_{n,m}]$ is between 0 and 1, and 1 otherwise. Another difference with Hall's work is that our approach is not limited to two and three cycle exchange, but includes all higher-order exchange effects. While four, five

and higher-order exchange cycles may not be significant at high temperature, our effective potential will give a realistic picture at lower temperature provided the number of nodes P is increased.

With an exchange potential defined, a molecular dynamics algorithm may now be applied to sample the states of a system containing ionic and electronic degrees of freedom. We note that a microcanonical ensemble sampling can be performed by averaging over the trajectories generated by the classical Hamiltonian

$$\begin{aligned} H = &\sum_{k=1}^{N_{\rm el}}\sum_{i=1}^{P}\frac{1}{2}m^*(\dot{\boldsymbol{r}}_i^{(k)})^2 + \sum_{I=1}^{N}\frac{1}{2}M_{\rm I}\dot{\boldsymbol{R}}_I^2 + \sum_{I>J}^{N}\sum_{I}^{N-1}\frac{Z_I Z_J}{4\pi\epsilon_0|\boldsymbol{R}_I-\boldsymbol{R}_J|} \\ &+\sum_{i}^{P}\sum_{k>l}^{N_{\rm el}}\sum_{l}^{N_{\rm el}-1}\frac{(-e)(-e/P)}{4\pi\epsilon_0|\boldsymbol{r}_i^{(k)}-\boldsymbol{r}_i^{(l)}|} + \sum_{i=1}^{P}\sum_{k=1}^{N_{\rm el}}\sum_{I=1}^{N}\frac{1}{P}V_{\rm pseudo}(\boldsymbol{R}_I-\boldsymbol{r}_i^{(k)}) \\ &+\sum_{k=1}^{N_{\rm el}}\sum_{i=1}^{P}\frac{m_e P}{2\overline{h}^2\beta^2}(\boldsymbol{r}_i^{(k)}-\boldsymbol{r}_{i+1}^{(k)})^2 - \frac{1}{\beta}\sum_{i=1}^{P}\sum_{j=1}^{P}\frac{1}{P}\ln(M[E_{ij}]\uparrow) \\ &-\frac{1}{\beta}\sum_{i=1}^{P}\sum_{j=1}^{P}\frac{1}{P}\ln(M[E_{ij}]\downarrow) \end{aligned} \tag{27}$$

where $M_{\rm I}$ are the ionic masses, m^* is some arbitrary mass attributed to the nodes [17] and N and $N_{\rm el}$ are the number of ions and electrons, respectively. The term $V_{\rm pseudo}$ is a pseudopotential describing the effective interaction between valence electrons and ions. As exchange can only take place between electrons with identical spins, the exchange potential is made spin-dependent by separating it into spin-up and spin-down parts. Furthermore, since our exchange potential is based on the assumptions that (i) most of the important configurations have $M[E_{n,m}] > 0$, and (ii) this potential offers an infinite energy barrier to configurations with negative $M[E_{n,m}]$, the electron trajectories will be biased toward configurations with positive determinants.

2.2. Model and practical implementation

We have successfully simulated a system constituted of 30 potassium ions and 30 valence electrons (15 with spin-up and 15 with spin-down) at a temperature of 1300 K. The mass m^* is taken to be equal to one atomic mass unit [17]. The simulation cell is a fixed cubic box with edge length $L = 13.3$ Å, which corresponds to the density of liquid potassium at the melting temperature [18]. The electron/potassium interaction is modelled with an empty core pseudopotential with a core radius $R_{\rm c} = 2.22$ Å [19]. The long-range Coulombic interaction is calculated via the Ewald summation method [20], with the Ewald parameter $\eta = 5.741/L$, and the real-space part of the summation truncated at $(1/2)L$. With this choice of parameters, the reciprocal-space sum in the Ewald construction is small compared to real-space contributions and may therefore be neglected [21].

To calculate the kinetic energy of the electrons, we use the energy estimator.

$$\begin{aligned} \langle KE\rangle = &\frac{3PN_{\rm el}}{2\beta} - \left\langle \sum_{j=1}^{N_{\rm el}}\sum_{i=1}^{P*}\frac{C}{2}(\boldsymbol{r}_i^{(j)}-\boldsymbol{r}_{i+1}^{(j)})^2\right\rangle \\ &+\left\langle \frac{\partial}{\partial\beta}\left(\sum_{m=1}^{P*}\sum_{n=1}^{P*}\frac{1}{P}(\ln(M[E_{n,m}]_\uparrow)+\ln(M[E_{n,m}]_\downarrow))\right)\right\rangle. \end{aligned} \tag{28}$$

This contribution to the energy is found by differentiating the partition function with respect to β, in the absence of electron interaction and external potentials.

Periodic boundary conditions are imposed on the system. Some care must be taken when using the exchange potential in equation (27) in association with periodic boundary conditions. For N electrons with identical spins, $[E_{n,m}]$ is a $N \times N$ matrix. The components $E^{ij}_{n,m}$ weigh a direct path along necklace (i) between imaginary times n and m versus an exchange path between necklaces (electrons) (i) and (j). We therefore construct the matrix $[E_{n,m}]$ by considering all pairs of electrons in the simulation cell (and image cells). Only those configurations of pairs of electrons which are most likely to contribute significantly to the partition function are selected. This is accomplished by selecting the pairs of electrons (i) and (j) for which $|(\boldsymbol{r}_n^{(i)}-\boldsymbol{r}_m^{(j)})^2+(\boldsymbol{r}_n^{(j)}-\boldsymbol{r}_m^{(i)})^2-(\boldsymbol{r}_n^{(i)}-\boldsymbol{r}_m^{(i)})^2-(\boldsymbol{r}_n^{(j)}-\boldsymbol{r}_m^{(j)})^2|$ is minimized. The justification for this is found in equation (22), where at high temperatures the second term is expected to dominate. Thus we choose a pair criterion for the construction of the matrix $[E_{n,m}]$.

The discretized path integral represents the exact quantum system when the number of nodes P tends to infinity. However, there exists a minimum value of P above which the properties of the classical system have nearly converged to the properties of the quantum system. In absence of exchange, the discretization of the electron is determined by the ratio of the potential energy of the electron to the thermal energy. In the case of electrons interacting with each other and with K^+ ions through an empty core pseudopotential, the potential energy is dominated by the electron Coulomb repulsion. The maximum potential energy may be calculated as $e^2/4\pi\varepsilon_0 r_{\min}$ where $r_{\min}$ is the minimum distance of approach between two interacting electrons. Within our cell the volume per electron is equal to $(4\pi/3)r_s^3$ where $r_s = 2.655$ Å (5.02 au). Taking $r_{\min} \sim r_s/2 = 1.32$ Å as a lower limit, the condition $P > e^2/4\pi\varepsilon_0 r_{\min} kT$ yields a lower bound for our system of approximately 100 nodes.

This value, however, may not ensure appropriate sampling of exchange-related states. An estimate of the minimum number of nodes for sampling exchanging states may be obtained by considering the limit of validity of our approximate partition function (equation (23)). This limit is reached when $(\boldsymbol{r}_n^{(i)} - \boldsymbol{r}_m^{(j)})^2$ and $(\boldsymbol{r}_n^{(j)} - \boldsymbol{r}_m^{(i)})^2$ in equation (22) are of the same order as $(\boldsymbol{r}_n^{(i)} - \boldsymbol{r}_m^{(i)})^2$ and $(\boldsymbol{r}_n^{(j)} - \boldsymbol{r}_m^{(j)})^2$. In other words, we want the equilibrium distance between the nodes n and m in the same necklace not to exceed the minimum distance between necklaces. We take the distance between necklaces as a measure of the distance for exchange. This distance is controlled by the Coulombic repulsion between electrons. We chose again $r_{\min} = 1.32$ Å as a lower bound. Since

$$\frac{Pm}{2\beta^2\hbar^2}(\boldsymbol{r}_n^{(i)} - \boldsymbol{r}_m^{(i)})^2 \sim \frac{3}{2\beta}$$

and setting $(\boldsymbol{r}_n^{(i)} - \boldsymbol{r}_m^{(i)})^2 \sim r_{\min}^2$, we get $P \sim 120$ nodes.

On this basis and on the basis of our previous work on solvation of four, six and eight electrons in molten potassium chloride at $T = 1300$ K, we choose a slightly higher number of nodes, $P = 150$ [22, 23].

Temperature is maintained constant during the simulation by using a momentum rescaling thermostat [24]. With this procedure we do not obtain a true canonical distribution, but most thermal averages will be accurate to order N^{-1} [25]. Furthermore, with 150 nodes and $T = 1300$ K, our simulations should equilibrate reasonably quickly as the intrapolymeric harmonic forces are not overly stiff [26]. Finally, although the electrons and ions are already in thermal equilibrium, we have found that employing one thermostat for the ionic species and one thermostat for each individual electronic necklace leads to even faster convergence.

For our system it is necessary to use a small integration time step to sample phase space accurately and produce stable trajectories. We solve the equations of motion with a finite-difference scheme with a time step of $\Delta t = 1.35 \times 10^{-16}$ s. This value allows us to run simulations long enough to sample a reasonable number of atomic states while still remaining computationally tractable. The exchange potential in equation (25), however, is very steep in some regions of configuration space. As a result, the forces derived from this potential have large values in these regions. This may lead to instabilities due to our choice of time step. In this case, measures have been taken to avoid any instability due to the large time step by restricting the exchange forces to an upper limit of 1.15×10^{-8} N. This upper limit was chosen such that the algorithm produces stable trajectories without significant loss of accuracy. In the algorithm, forces exceeding the upper limit are renormalized to the upper limit value.

We verified that the number of nodes subjected to exchange forces larger than our upper limit represents only a very small fraction of all of the nodes in the simulation cell. We also verified that at any given time during a simulation, the large majority of forces exceeding the upper limit do so only by at most a factor of three. Furthermore, a simulation conducted with an upper limit of 2.3×10^{-8} N did not show any significant change in the average electron kinetic energy to within the uncertainty.

3. Results and discussion

A random distribution of nodes and ions was created as starting configuration for a preliminary simulation limited to harmonic potentials between nodes. This simulation produced an equilibrated configuration which was then used as an initial condition for all subsequent simulations. Three simulations were run. This first simulation lasted 10 000 integration time steps or approximately 1.3×10^{-12} s and included quantum exchange. A second simulation of free electrons without exchange was conducted by ignoring all the interaction terms in equation (27), excluding the effective harmonic potential between neighboring nodes. The third simulation consisted of a system of interacting electrons in liquid potassium without exchange. This system is simulated by removing the effective nonlocal exchange potential from the Hamiltonian. Both the second and third simulations lasted 20 000 steps. We report in figure 1 the instantaneous value of the kinetic energy per electron for the first simulation. The initial 2500 steps were discarded as a transient period and a time average was calculated over the remaining 7500 steps. The calculated average kinetic energy per electron is presented in table 1. Table 1 also includes the kinetic energy of free electrons in absence of an exchange potential, free electrons with exchange and the kinetic energy of interacting electrons in liquid potassium in absence of exchange. The kinetic energy of the free electrons with exchange is obtained from the expression $2.21/r_s^2$ (Ryd) [27], with $r_s = 5.02$ au. Both kinetic energies in absence of exchange are computed as time averages in simulations (2) and (3). Finally, we have added in table 1, the result of Pines and Nozieres [28] for the kinetic energy of non-interacting electrons in a potassium periodic potential at a density of $r_s = 4.87$ au.

The electron localization due to electron–electron and electron–ion Coulomb interaction in the absence of the exchange potential is associated with a kinetic energy approximately equal to $\frac{2}{5}$ eV. Upon introduction of the fermionic constraint through the effective exchange potential, the kinetic energy increases to 1.73 eV. This increase of 1.34 eV is in good accord with the difference in kinetic energy of 1.2 eV between the free-electron system with and without exchange. One may therefore view interacting electrons in liquid potassium within a quasi-particle representation with a zero of energy at $\frac{2}{5}$ eV. The positive difference in

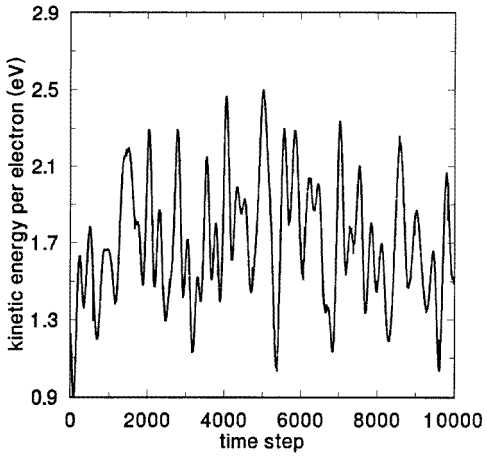

Figure 1. Electronic kinetic energy against time (one time step equals 1.34×10^{-16} s). The kinetic energy of interacting electrons with exchange potential in liquid potassium at $T = 1300$ K is calculated using the energy estimator of equation (28).

Table 1. Electronic kinetic energy for various systems. See text for details.

System	Kinetic energy per electron (eV)
Free electrons without exchange	0.00 ± 0.01
Liquid potassium with interacting electrons in absence of exchange	0.39 ± 0.05
Free electrons with exchange	1.19
Non-interacting electrons in periodic potential including exchange	1.42
Liquid potassium with interacting electrons including exchange	1.73 ± 0.05

kinetic energy between our liquid potassium and the results of Pines and Nozieres for crystalline potassium may be attributed to additional electron localization resulting from the electron–electron repulsion and the disordered arrangement of the potassium ions in the liquid phase. Further localization may also arise from atomic vibration [29] which is intrinsic in our simulation.

The electronic structure of liquid potassium is best illustrated by the electron–ion and electron–electron radial distributions. Figure 2 shows that the electrons are concentrating on the periphery of the ionic core. The fact that the electrons are not localized within each ion is indicative of the participation of electrons in bonding. In figure 3, we have plotted the electron–electron distribution for isospin and heterospin electrons. Coulombic repulsion prevents electrons from approaching one another for distances less than 1 Å. The choice for $P > 120$ based on a minimum distance of approach of 1.32 Å appears then to be quite reasonable. Apart from illustrating the effect of the Coulomb repulsion, this figure shows the effectiveness of the non-local exchange potential in ensuring Pauli exclusion principle. The exclusion is particularly active between 1 and 5 Å with an isospin electron probability reduced by almost a factor of two for distances less than r_s. The overlap between the two distributions beyond 6 Å suggests that in liquid potassium the non-local exchange potential is reasonably short range.

Finally, figure 4 illustrates the calculated pair distribution function of liquid potassium at

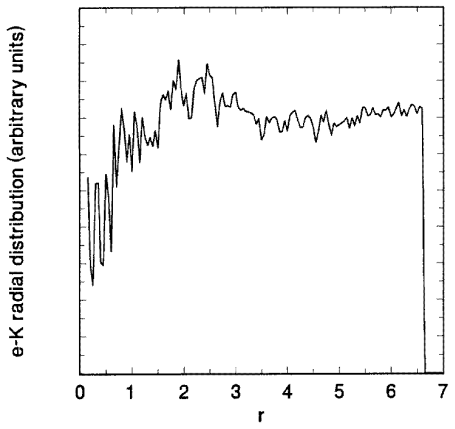

Figure 2. Average electron–ion radial distribution. The radial distance is in units of ångströms.

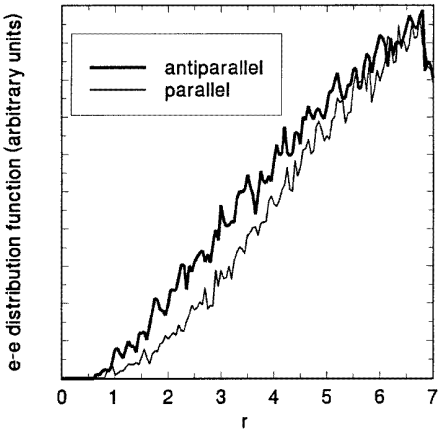

Figure 3. Average electron–electron radial distribution. The thick and thin curves correspond to heterospin and isospin electrons, respectively. The radial distance is in ångströms.

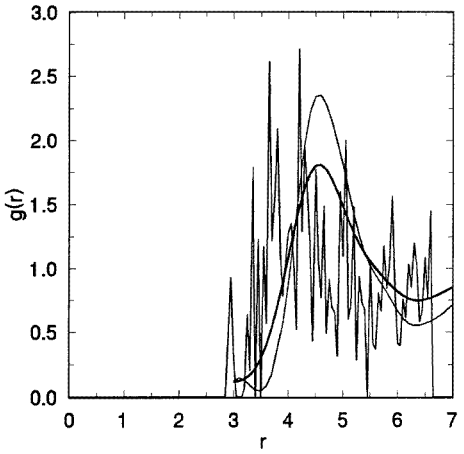

Figure 4. Calculated ion pair distribution function at $T = 1300$ K. The thick and thin continuous curves are the experimental data of Waseda [30] at 343 K and 723 K, respectively. The radial distance is in ångströms.

1300 K as well as the experimentally determined distribution functions at 343 K and 723 K [30]. The short length of our simulation and the small cell size are at the origin of the scatter in the calculated distribution. Despite this noise, one can identify three significant features. The radial distribution function exhibits three groups of peaks near 3.8 Å, 4.3 Å, and 5 Å. Close analysis indicates that the sharp peaks near 3.8 Å are associated with potassium dimers, K_2. First, this calculated separation is in good accord with the experimental value of 3.923 Å for the K_2 molecule [31]. Second, a molecular dynamics simulation of two potassium ions and two heterospin electrons at 1300 K confirmed the formation of a molecule with an average separation distance in the vicinity of 3.8 Å. Finally, the presence of K_2 dimers is clearly apparent in the snapshot of the simulation cell taken near the end of the simulation

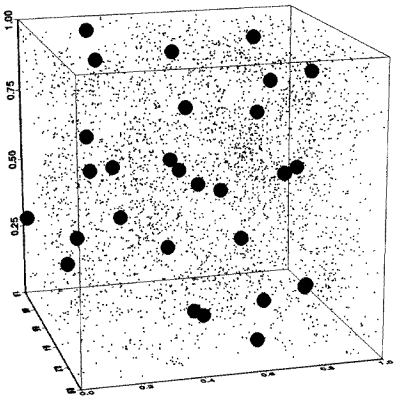

Figure 5. Snapshot of the simulation cell at time step 10 000. The large black circles are the potassium ions. Each small dot represents a node on an electron necklace. The length of a cell's edge is 13.3 Å.

and presented in figure 5.

The formation of diatomic molecules may be explained by the high temperature of the simulation which will favor the dissociation of large potassium clusters to form smaller ones. To verify this hypothesis, we have frozen the liquid to room temperature and relaxed it at this temperature for 2500 time steps. In order to ensure the conditions of validity for the exchange potential in our Hamiltonian, we have maintained the electrons at a temperature of 1300 K while decreasing the temperature of the ionic degrees of freedom to 300 K. This procedure is made possible by the separate thermalization of the electrons and ions. Since temperature variations in the interval 300–1300 K are not anticipated to affect significantly the electronic states, this method would effectively result in a cooling of the liquid and a reduction in the ion displacements. The calculated radial distribution function in figure 6 shows that the peaks near 3.8 Å (indicative of molecular K_2) are reduced significantly. This observation suggests that the features around 4.3 Å and 5 Å are the only ones characteristic of large size potassium clusters.

Larger potassium structures in the $T = 1300$ K liquid may be identified in figure 5. However, since this figure represents an instantaneous configuration with all possible thermal distortions the nature of these structures cannot be resolved. To gain some insight into the structure of liquid potassium we treat it as resulting from distortions of ideal crystalline structures. In a body centered cubic (bcc) structure, the second-nearest neighbor distance, d_2 is only slightly larger than the first-neighbor distance, d_1. In an ideal bcc lattice, $d_2^{\mathrm{bcc}} = 2d_1/\sqrt{3}$. On the other hand, a face-centered cubic (fcc) structure possesses two well resolved first and second neighbor shells with $d_2^{\mathrm{fcc}} = d_1\sqrt{2}$. Thus, to identify the structure of the simulated liquid as bcc-like or fcc-like, we take $d_1 = 4.3$ Å and calculate $d_2^{\mathrm{bcc}} = 4.96$ Å and $d_2^{\mathrm{fcc}} = 6.08$ Å. The presence of peaks near 5 Å in the pair distribution of the liquid (figure 4) supports a bcc-like liquid structure reminiscent of the crystal structure.

Finally, we note that the peaks in figure 4 near 4.3 Å and 5 Å are artificially narrowed. The small number of particles in the simulation cell and the short time of the simulations do not allow for a complete sampling of atomic configurations (in particular large clusters). A broadening and overlap of these peaks for larger systems should lead to a better fit with experimental radial distribution functions.

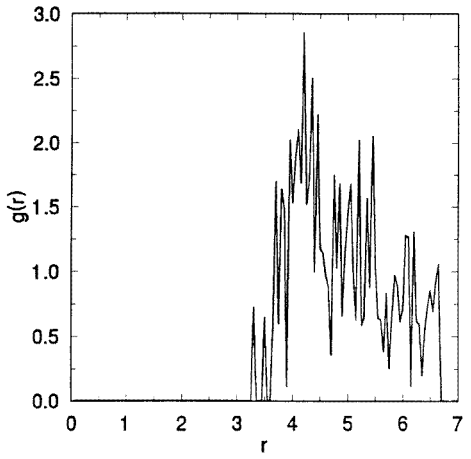

Figure 6. Calculated ion pair distribution function at $T = 300$ K. The radial distance is in ångströms.

4. Conclusions

We have developed and implemented a first-principle molecular dynamics method based on the discretized path integral formulation of quantum mechanics. Our approach uses an effective potential to model the effect of quantum exchange. This method has been employed to simulate liquid potassium. The calculated energies and structures are in satisfactory agreement with experimental as well as other theoretical results. The exchange potential appears to be quite efficient at enforcing the Pauli exclusion principle.

In the path integral molecular dynamics method, the computing time for the calculation of the exchange forces scales as P^2N^3 where N is the number of isospin electrons and P is the number of discrete states (nodes). This poor scaling with system size currently restricts the applicability of the method to systems containing a small number of electrons. It may be possible, however, to take advantage of the short-range nature of exchange to achieve a better scaling [32]. For instance, a large simulation cell may be divided up into subcells whose size is determined by some appropriate cut-off length. Consequently, the number of operations would reduce to P^2M^3N where M is the number of isospin electrons in a subcell. Another problem, which limits the applicability of this method to high temperature is the P^2 factor in computational cost. A proposed solution involves parallelization over the nodes [33], which leads to linear scaling. Simulations at lower temperatures will require a larger number of nodes resulting in non-ergodic behavior of the necklaces. A solution to this problem has been proposed recently in the form of a chain of Nosé–Hoover thermostats [34, 35].

As a final note, the electron–ion pseudopotential employed in this study is local in nature, however, the extension of the path integral molecular dynamics method to systems of electrons interacting with ions through non-local pseudopotentials may be accomplished by using a recently developed expression for the discretized path integral in polar coordinates [36].

References

[1] Ciccotti G, Frenkel D and McDonald I R (ed) 1987 *Simulation of Liquids and Solids* (Amsterdam: North-Holland)
[2] Car R and Parrinello M 1985 *Phys. Rev. Lett.* **55** 2471
[3] Lynch D L, Trouillier N, Kress J D and Collins L A 1994 *J. Chem. Phys.* **101** 7048
[4] Guo-Xin Qian, Weinert M, Fernando G W and Davenport J W 1990 *Phys. Rev. Lett.* **64** 1146
[5] Stratt R M 1990 *Ann. Rev. Phys. Chem.* **41** 175
[6] Freyland W 1979 *Phys. Rev.* B **20** 5104
[7] Hernandez J P 1986 *Phys. Rev. Lett.* **57** 3183
[8] Barker J A 1974 *J. Chem. Phys.* **70** 2914
[9] Chandler D and Wolynes P G 1981 *J. Chem. Phys.* **74** 4078
[10] Hall R W 1988 *J. Chem. Phys.* **89** 4212
[11] Hall R W 1989 *J. Phys. Chem.* **93** 5628
[12] Hall R W 1989 *J. Chem. Phys.* **91** 1926
[13] Feynman R P 1965 *Quantum Mechanics and Path Integrals* (New York: McGraw-Hill)
Feynman R P 1972 *Statistical Mechanics* (New York: Benjamin)
[14] Kleinert H 1990 *Path Integrals in Quantum Mechanics, Statistics, and Polymer Physics* (Singapore: World Scientific)
[15] Takahashi M and Imada N 1984 *J. Phys. Soc. Japan* **53** 963
[16] Ceperley D M 1992 *Phys. Rev. Lett.* **69** 331
[17] Parrinello M and Rahman A 1984 *J. Chem. Phys.* **80** 860
[18] Smithells C J 1992 *Metals Reference Book* 7th edn (London: Butterworth)
[19] Harrison W A 1966 *Pseudopotentials in the Theory of Metals* (New York: Benjamin)
[20] Kittel C 1986 *Introduction to Solid State Physics* 6th edn (New York: Wiley)
[21] Linse P and Anderson H C 1986 *J. Chem. Phys.* **85** 3027
[22] Iyer V, Jabbour G E, Deymier P A and Lee C Y 1993 *Modelling Simulation Mater. Sci. Eng.* **1** 361
[23] Jabbour G E 1994 *PhD Dissertation* University of Arizona
[24] Woodcock L V 1971 *Chem. Phys. Lett.* **10** 257
[25] Gillan M J 1990 *Computer Modelling of Fluids, Polymers and Solids* ed C R A Catlow *et al* (Dordrecht: Kluwer Academic) p 155
[26] Hall R W and Berne B J 1984 *J. Chem. Phys.* **81** 3641
[27] Ashcroft N W and Mermin N D 1976 *Solid State Physics* (Holt-Saunders Int. Editions)
[28] Pines D and Nozieres P 1989 *The Theory of Quantum Liquids: Normal Fermi Liquids* (Reading, MA: Addison-Wesley)
[29] Hall R W 1990 *J. Chem. Phys.* **93** 8211
[30] Waseda Y 1980 *The Structure of Non-Crystalline Materials* (New York: McGraw-Hill)
[31] Herzberg G 1950 *Molecular Spectra and Molecular Structure. I. Spectra of Diatomic Molecules* (New York: Van Nostrand)
[32] Li X-P, Numes R W and Vanderbilt D 1993 *Phys. Rev.* B **47** 10 891
[33] Marx D and Parrinello M 1994 *Z. Phys.* B **95** 143
[34] Martyna G J, Klein M L and Tuckerman M 1992 *J. Chem. Phys.* **97** 2635
[35] Tuckerman M E, Berne B J, Martyna G J and Klein M L 1993 *J. Chem. Phys.* **99** 2796
[36] Jabbour G E and Deymier P A 1994 *Modelling Simulation Mater. Sci. Eng.* **2** 1111